First Success in Direct Analysis of Microscopic Deformation Mechanism of Polydiacetylene Single Crystal by the X-ray Imaging-Plate System

Kohji Tashiro,* Hirokazu Nishimura, and Masamichi Kobayashi

Department of Macromolecular Science, Faculty of Science, Osaka University, Toyonaka, Osaka 560, Japan

Received June 18, 1996; Revised Manuscript Received August 22, 1996[⊗]

ABSTRACT: The deformation mechanism of a polymer crystal has been directly clarified for the first time using an imaging-plate X-ray structural analysis system for a polydiacetylene single crystal subjected to a tensile stress at room temperature as well as at 122 K. That is to say, the small displacements of the constituent atoms of the planar-zigzag skeletal chain could be successfully detected. The change in the internal coordinates such as bond length and bond angle, which were induced by tensile stress, has been found to be consistent with the previously reported lattice-dynamical prediction. This first success in the accurate structural analysis of the deformed polymer crystal is considered to supply a new technique for investigating the deformation mechanism of polymer materials from the molecular level.

Introduction

It is very important to understand the mechanical properties of polymers from the molecular level so as to modify and/or predict those of new polymer substances. Unfortunately, however, it is quite difficult to investigate the relationship between the mechanical properties and structure of the bulk samples which consist of the complicated aggregation of both the crystalline and amorphous phases. One of the most effective and useful methods may be an approach to the crystalline phase with a regular structure which might be assumed as a limiting state of the bulk polymer samples. In a series of papers[1] we have tried to understand the intimate relationship between the structure and mechanical properties on the basis of the lattice dynamics and energy calculation techniques. The lattice dynamics can predict the atomic displacements induced by the externally applied force, from which the elastic constants can be understood reasonably and quantitatively in connection with the chain conformation and the packing state of the chains.

This theoretically-predicted atomic displacement, in other words, the mechanical deformation mechanism, should be proved experimentally. The vibrational spectroscopy or the infrared and Raman scattering methods can supply very important information on the atomic displacements in a form of the vibrational frequency shifts, which are induced by an application of a stress or strain to the sample.[2−12] Among the many bands observed in the spectra, mostly only the bands of the skeletal vibrational modes shift to the lower frequency side when the sample is tensioned along the chain axis. On the basis of the lattice-dynamical theory developed under a quasiharmonic approximation, we were able to clarify the quantitative relationship between the frequency shifts and the atomic displacements by assuming that the force constants are modified through the changes in the internal coordinates, such as the bond lengths, bond angles, and/or internal torsional angles.[9−12] This idea has been applied actually to the cases of poly(oxymethylene), isotactic polypropylene, and orthorhombic polyethylene crystal with satisfactory reproduction of the observed spectral changes.[9−12]

At this stage, however, we have to realize that the vibrational spectroscopic interpretation of the mechanically deformed polymer crystals has a limitation in getting direct information concerning the atomic displacements. This is because the vibrational frequency is a function of the force constants and the atomic coordinates in a complicated manner. In order to obtain more direct and definite information concerning the atomic displacements, we have to necessarily rely on the refined crystal structural analysis by using the X-ray diffraction technique. In general the polymer crystals show quite poor X-ray diffraction patterns consisting of a small number of broad reflections, making it difficult to utilize the "direct" method employed frequently in the refined structural analysis of low-molecular-weight compounds. This situation makes it practically impossible to detect the quite small atomic displacements occurring in the deformed polymer crystal. We need to obtain a single crystal of polymer which is large enough to be treatable by hand. As is well-known the polymer single crystals are in general very small with a submicron size at most, which cannot be used for the present purpose. Fortunately, however, we have one exception: it is polydiacetylene which is obtained by solid-state polymerization of the monomer single crystal. In a previous paper[8] we used the polydiacetylene single crystal with carbazolyl groups as side chains, poly[1,6-di(*N*-carbazolyl)-2,4-hexadiyne] (PDCHD), in the infrared and Raman spectroscopic measurements under tension at the various temperatures. The sample is about several centimeters in length and several hundred micrometers in width, as shown in Figure 1. In the present study we will utilize this PDCHD single crystal as a candidate for the abovementioned purpose, i.e., an experimental proof of molecular deformation mechanism. Concretely speaking, this PDCHD sample is tensioned uniaxially by using the homemade stretcher, which is mounted on the goniometer head, and then the sets of X-ray oscillation photographs are taken. The X-ray diffraction data are collected by using the recently developed imaging-plate (IP) system, which has been found to be very useful for the structural analysis of single crystals such as protein and low-molecular-weight compounds as well as for the structural study of polymer materials. The refined structural analysis is made for the collected IP data and

[⊗] Abstract published in *Advance ACS Abstracts,* November 1, 1996.

S0024-9297(96)00882-0 CCC: $12.00

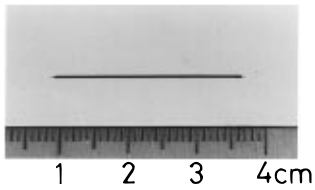

Figure 1. Photograph of the PDCHD giant single crystal. The scale between a couple of major ticks is 1 cm.

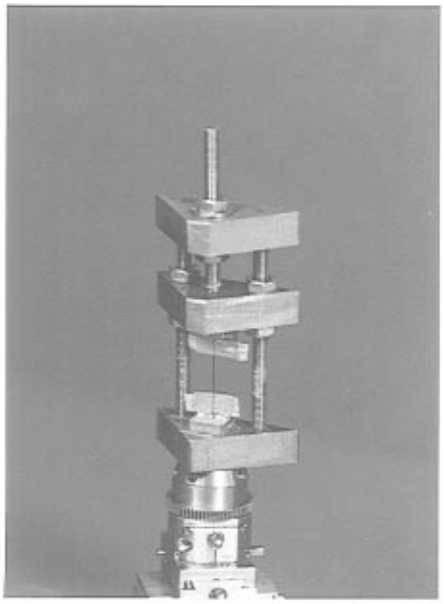

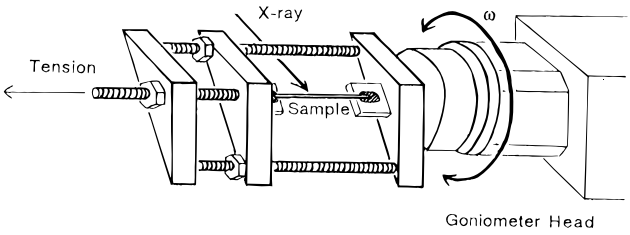

Figure 2. Illustration of sample stretcher and its real photograph.

the change in the unit cell parameters; the atomic positions will be evaluated as well. On the basis of the clarified structural data as a function of tensile strain, the deformation mechanism of the PDCHD crystal will be discussed in detail. This may be the first success for synthetic polymers in getting such detailed information on the deformation mechanism viewed from the molecular level.

Experimental Section

Samples. Needlelike single crystals of diacetylene (DCHD) monomer were grown slowly from a toluene solution at room temperature.[8] These single crystals were polymerized in the solid state by an irradiation of ^{60}Co γ-ray (40 Mrad) at room temperature. Thus obtained PDCHD single crystals have a needlelike shape with a dimension of 30 mm length and 0.1 mm width, as shown in Figure 1. The uniform single crystals were picked out under the optical microscope and supplied to the X-ray diffraction experiment. The cross-sectional area of the crystal is homogeneous, allowing us to apply uniform stress (or strain) over the whole sample.

Application of Tension onto a Crystal. The thus obtained PDCHD single crystal was set into the homemade sample stretcher, as shown in Figure 2. Both ends of the sample were fixed in the holder, and the sample was strained

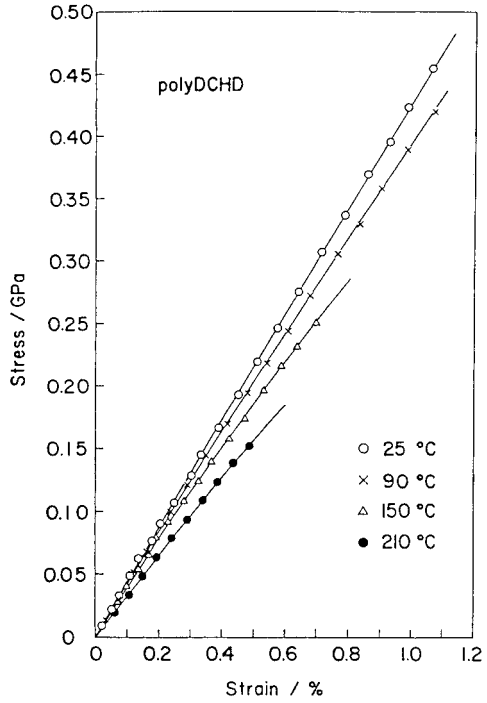

Figure 3. Stress−strain curves of the PDCHD giant single crystal measured at the various temperatures.[8]

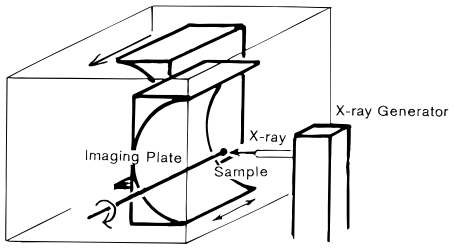

Figure 4. Illustration of the camera section of the DIP3000 X-ray diffraction system (referred to in the text).

by moving the one end of the holder by careful rotation of the screw. One of the most important points of this experiment was how to fix the sample tightly onto the stretcher. The sample was attached strongly to the metal of the holder by adhesives. The length of the sample fixed by adhesives must be long enough to perfectly suppress the slippage of the sample along the stretching direction. The sample was placed under tension at a constant strain, during which the X-ray measurement was made. The tensile strain was less than 1% at most. At this stage we note that in the case of general synthetic polymers some stress relaxation occurs frequently when the samples are subjected to the constant *strain*, which might make the strain behavior ambiguous because of the stress relaxation during the experiment. In the case of the PDCHD single crystal, however, such stress relaxation may not be considered to occur, because the stress−strain relation obeys almost perfectly the so-called Hookian law, as shown in Figure 3;[8] in other words, this polymer crystal is considered to exhibit the almost perfect energy elasticity at room temperature.

X-ray Measurements. The X-ray diffraction data were collected by using an IP system DIP3000 developed by MAC Science, Ltd. An illustrative picture of the system is shown in Figure 4. The κ-goniometer is installed on the X-ray generator (rotating-anode-type SRA-M18XHF, maximal voltage 60 kV and maximal current 300 mA). This DIP3000 has two cylindrical cameras (15 cm in radius) which are used alternately and repeatedly: a photograph is taken by one camera at the front side; the other camera is operated so as to read the accumulated data at the opposite back side. The IP system was chosen for the present experiment because the IP gives a two-dimensional X-ray diffraction pattern, so we need to oscillate the sample around only one axis (ω axis),, enabling us to mount the sample stretcher. This is quite in

Table 1. Comparison of Lattice Parameters of the Cytidine Single Crystal Obtained by the Various X-ray Diffraction Measurements

installment[a]	*a*/Å	*b*/Å	*c*/Å
AFC5R	14.008	14.790	5.123
AFC5R	14.015	14.791	5.120
AFC7R	13.977	14.763	5.114
κ-gonio	14.004	14.776	5.116
Guinier	13.991	14.786	5.116
DIP3000	14.014	14.801	5.124
DIP3000	14.011	14.798	5.123
DIP3000	14.012	14.799	5.123
DIP3000	14.012	14.801	5.122
DIP3000(β)	13.970	14.755	5.108
DIP1000	14.015	14.795	5.122
mean (all)[b]	14.003	14.787	5.118
σ	±0.016	±0.016	±0.006
σ/mean	±0.001	±0.001	±0.001
mean (DIP3000)	14.004	14.791	5.120
σ	±0.019	±0.020	±0.007
σ/mean	±0.001	±0.001	±0.001

[a] AFC5R, AFC7R, Automatic four-circle X-ray diffractometer (Rigaku); κ-gonio, κ-Goniometer (Nonius); Guinier, Guinier camera;[36] DIP3000, MAC Science; DIP3000 (β), Mo Kβ line used; DIP1000, MAC Science. [b] Mean (all), mean values averaged for all of the data; mean (DIP3000), mean values averaged for the data of DIP3000; σ, standard deviation.

contrast to the situation of an automatic four-circle diffractometer in which the sample has to be rotated in a complex manner around the ϕ and χ axes (the ϕ axis is a spindle axis of the sample, and the χ axis is a tilt angle along the meridional line), making it difficult to hold the relatively heavy and bulk sample stretcher.

The sample stretcher was mounted on the goniometer head of the X-ray diffraction installment and the longest axis of the sample, i.e.; the chain axis was adjusted so as to coincide with the spindle (ϕ) axis of the goniometer (see Figure 2). A total 20 shots of quasi-Weissenberg photographs with an oscillation angle ($\Delta\omega$) of 5° and a translation width of 1 cm were taken in the range of $\omega = 0-100°$ at a constant strain, where a graphite-monochromatized Mo Kα radiation ($\lambda = 0.710\ 73$ Å) was used as an incident X-ray source (50 kV, 200 mA). The 5−7 sets of 20 Weissenberg photographs were taken for the sample with the same strain in order to evaluate the accuracy of the analyzed results and the experimental errors. The exposure time of one shot was 10 min and only about 3.5 h was needed so as to collect a set of photographs. (This should be compared with the case of the automatic four-circle diffractometer in which the full collection of the data was made in about 24 h in the case of PDCHD.)

Structural Analysis. The collected X-ray photographs were analyzed after the data were transferred from the workstation (SUN Sparc2) as an X-ray machine controller to the Silicon Graphics Indigo2 workstation through the network. For the indexing of the reflections and the integration of the intensity, computer softwares "DENZO", developed by Z. Otwinowski,[13] and "XDISPLAYF", developed by W. Minor,[14] were used. The DENZO can index the diffraction pattern, and refine the crystal lattice parameters and the detector parameters such as the rotation axis of the sample, the center position of the oscillation, etc., and integrate the diffraction intensity. The XDISPLAYF can compare the observed IP pattern with the reflection spots calculated by using the fitted parameters which are obtained and refined in the course of data analysis by DENZO. The total number of the observed reflections was about 6000, from which the effective and independent reflections, about 2300, were extracted ($0 < h < 18$, $0 < k < 4$, and $-24 < l < 23$). On the basis of the thus collected reflectional data, another software "SCALEPACK" (developed by Z. Otwinowski) was used so as to determine the more accurate lattice parameters and the scale factors between the successive frames of photograph, from which the exactly corrected data of the structure factor were obtained[15]. The structural analysis through the direct method was made on the basis of MULTAN78.[16] Least-squares refinement was made on the basis of the full matrix method by using the quantity $\sum w(|F_o|^2 - |F_c|^2)^2$ as a minimized function with the weight $w = \exp[FA \sin^2 \theta/(\lambda^2\sigma^2(F_o))]$, where $\sigma^2(F_o)$ is the squared standard error of the observed structure factor and the coefficient FA was set to the value 0.001. The reflections used in the least-squares calculation were about 1300 with the data reduction cutoff of $|F_o| \geq 3\sigma(|F_o|)$. Final reliability factors were $R = 0.04-0.05$ and $R_w = 0.04-0.05$ for all of the samples, where the R and R_w are defined as follows: $R = \sum||F_o| - |F_c||/\sum|F_o|$ and $R_w = [\sum w(|F_o| - |F_c|)^2/\sum w|F_o|^2$. All of the data of R, R_w, the number of observed unique reflections, and the

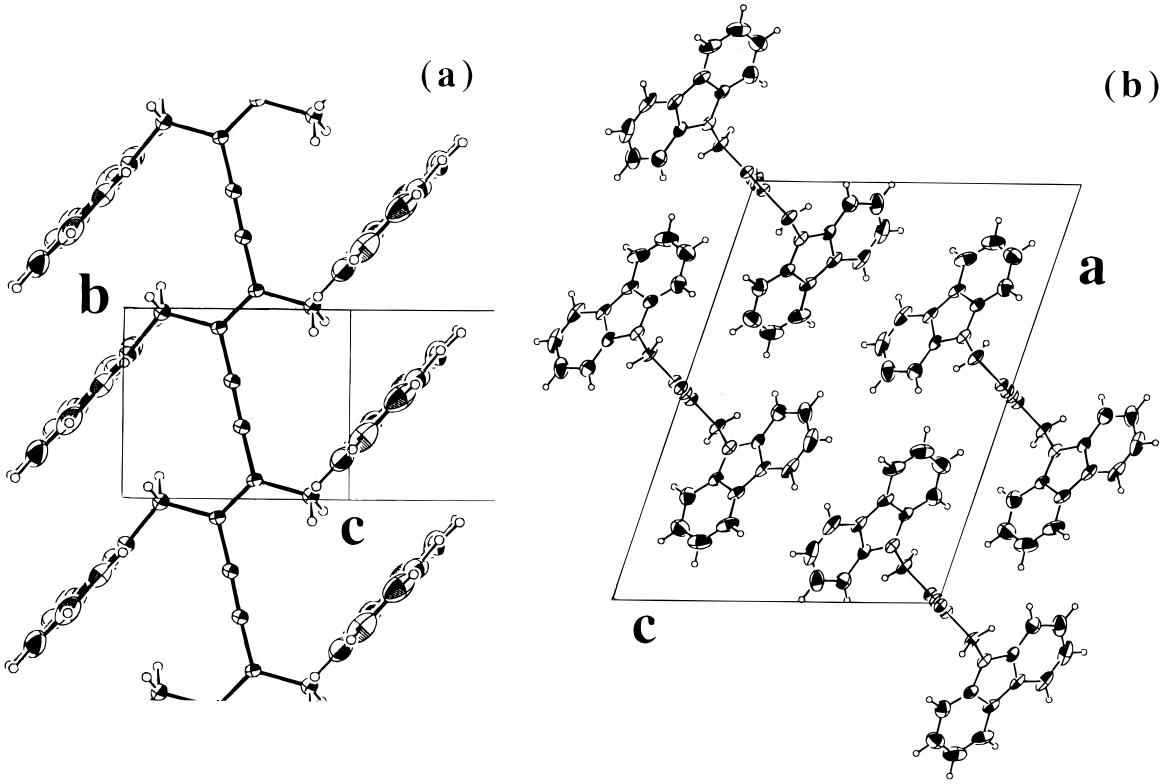

Figure 5. (a) Molecular and (b) crystal structures of PDCHD in the strain free state.

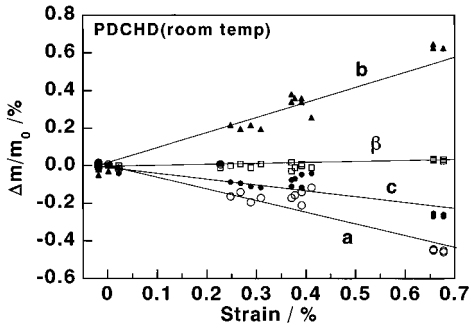

Figure 6. Stress-induced changes of lattice parameters plotted against the strain (room temperature).

numbers of reflections used in the refinements are listed in the table presented as Supporting Information.

Results and Discussion

Evaluation of Accuracy of Structural Analysis by the DIP3000 System. The IP system used here was developed about five years ago and is now being spread over the world because of its high sensitivity to X-ray beam and its wide dynamic range of intensity evaluation (covering $1-10^6$ photons).[17−19] In particular the DIP3000, produced by MAC Science, was developed so as to collect the X-ray reflection data in a Weissenberg type which can separate the accidentally overlapped reflections with different *hkl* indices by the translation of the camera along the rotation axis. This installment includes a couple of cylindrical IP cameras of 15 cm radius, and the measurement and the data processing can be made alternatively and continuously by exchanging these two cameras. In order to check the accuracy of structural analysis made by using this new system, we measured the six to seven independent sets of oscillation or Weissenberg photographs for a standard single crystal cytidine and analyzed the structure following the process mentioned in the Experimental Section. The obtained structural information of cytidine is listed in Table 1 in which the lattice parameters are compared among the different sets of data including the results obtained by the automatic four-circle diffractometer and those reported by other researchers.[20] (It should be noted here that in this experiment only one single crystal of cytidine was used. This is because even the "apparently same" single crystals obtained from the same source might give, strictly speaking, diffraction data of different quality. Besides, even when just the same crystal was used, the scattering geometry, etc., might be changed if the setting condition was changed in every experiment. This may affect the accuracy of the internal parameters because the scattering power at high angle, for example, might be changed due to such a geometrical problem. Therefore the results on such internal parameters as bond length, bond angle, etc., are listed only as a reference in the tables of the Supporting Information.) The averaged unit cell parameters of cytidine are as follows: the space group $P2_12_12_1$ and the orthorhombic cell with $a = 14.000 \pm 0.016$ Å, $b = 14.786 \pm 0.014$ Å, and $c = 5.118 \pm 0.006$ Å. As seen in Table 1, the ratio of standard error to the mean value is about 10^{-3} for the lattice parameters (and about 3×10^{-3} for the internal coordinates such as bond lengths, bond angles, and so on). That is to say, we may discuss the structure of a crystal with a significant confidence of an order of 10^{-3}. On the basis of this structural accuracy we will discuss the structural change of PDCHD induced by an externally applied stress, as described in the following sections.

Strain-Induced Change of Unit Cell Parameters of PDCHD. In Figure 5 are shown the molecular and crystal structures of PDCHD at the strain free state, which were obtained by the above-mentioned X-ray system. The cell parameters averaged over the seven independent results are $\langle a \rangle = 12.846 \pm 0.001$ Å, $\langle b \rangle$ (fiber axis) $= 4.887 \pm 0.001$ Å, $\langle c \rangle = 17.332 \pm 0.004$ Å, and $\langle \beta \rangle = 108.30 \pm 0.01°$. The space group is $P2_1/c-C_{2h}^5$. The averaged reliability factor $\langle R \rangle = 5.0\%$. The thus analyzed structure is essentially the same as that reported by Apgar and Yee[21] in 1978, although the number of

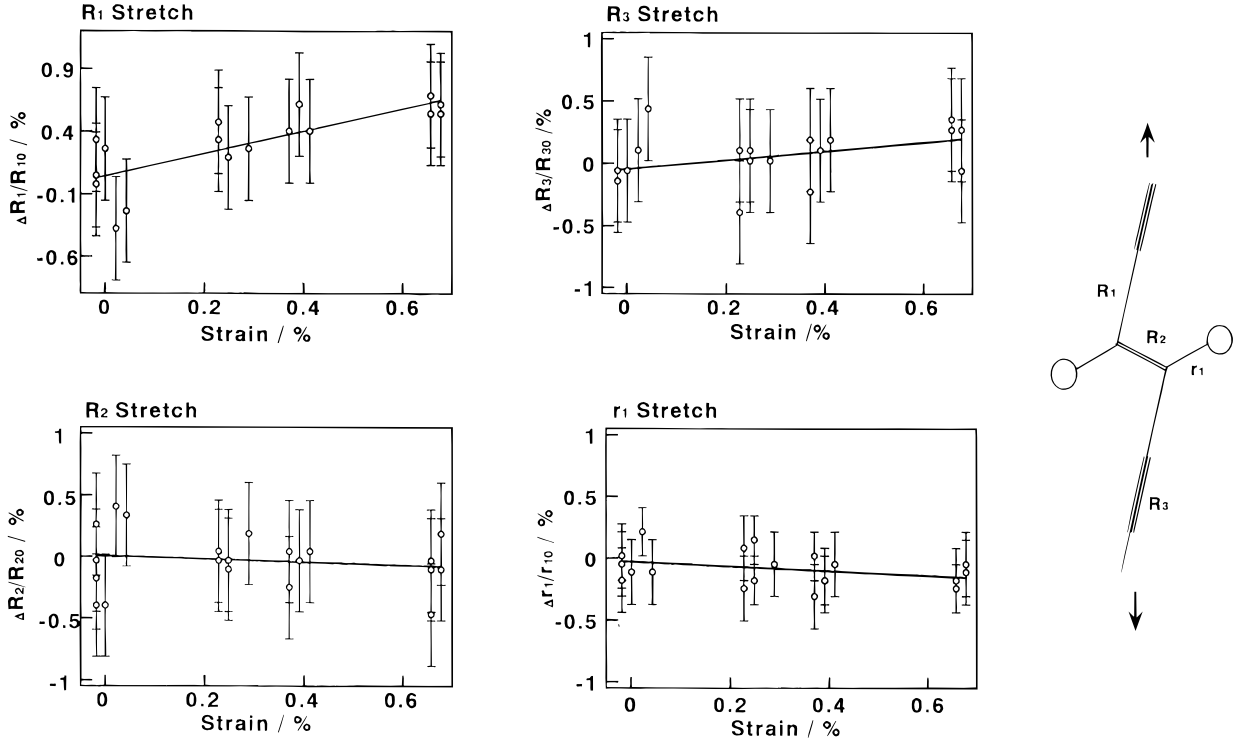

Figure 7. Strain dependence of bond lengths of the PDCHD chain (room temperature). The definition of the bond lengths is made in the right side of this figure.

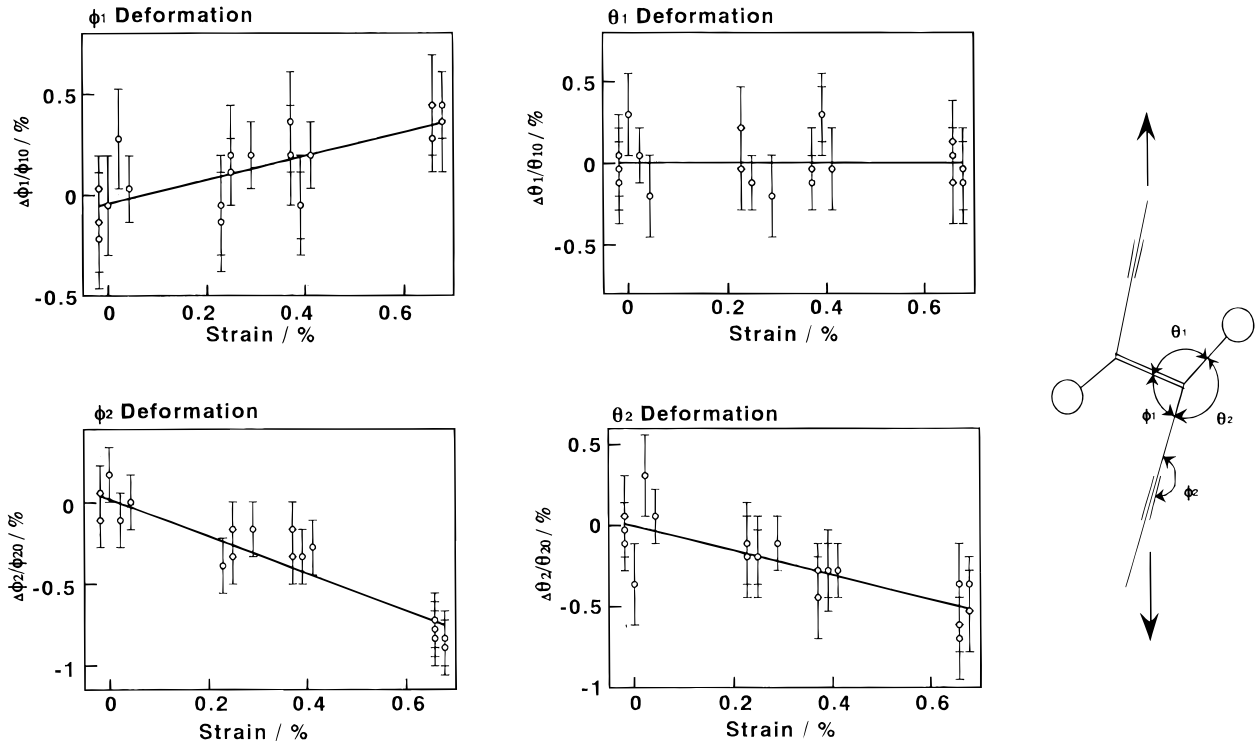

Figure 8. Strain dependence of bond angles of the PDCHD chain (room temperature). The definition of the bond angles is made in the right side of this figure.

observed reflections is more and the reliability factor is better in the present case using the IP system. As seen in Figure 5, the molecular chain takes essentially the fully extended all-trans conformation, and the carbazolyl side-chain groups are packed well in a herringbone structure. In Tables 2 and 3 are shown, respectively, the fractional coordinates of the constituent atoms and the internal structure parameters of PDCHD at the strain free state.

At the stage where the accuracy of the system was established quantitatively, we proceeded to the next stage of stretching the PDCHD sample. The crystal was stretched at a constant strain, during which a set of Weissenberg photographs was taken at room temperature. This process was repeated six to seven times at almost the same strain value. The reflections do not split into several pieces under tension, indicating that the crystal was not broken but was deformed in a recoverable elastic strain range. The change in the lattice parameters evaluated from these data are listed as follows

strain/%	*a*/Å	*b*/Å	*c*/Å	*β*/deg
0.0	12.846	4.887	17.332	108.30
0.25	12.826	4.899	17.317	108.30
0.39	12.824	4.906	17.318	108.30
0.67	12.788	4.919	17.286	108.33

and also plotted against the applied strain as shown in Figure 6, where the changes are represented by percentages with the parameters obtained at the free strain as initial values (the strain along the chain axis is calculated as $(b - b_o)/b_o$, where the *b*-axial value averaged for all the date obtained at free strain states was used as b_o). As the fiber axis *b* is increased by tension, the *a* and *c* axes are contracted but the angle *β* does not change very much. These strain-induced changes in the cell constants are reversible almost perfectly. This can also be said for the changes in the internal parameters, as discussed in Figures 7 and 8 and so on in a later section. From these data we may

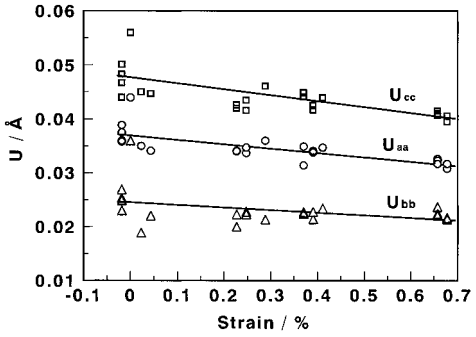

Figure 9. Strain dependence of the diagonal components of the anisotropic thermal parameters of the carbon atom (C1) of the PDCHD skeletal chain evaluated at room temperature.

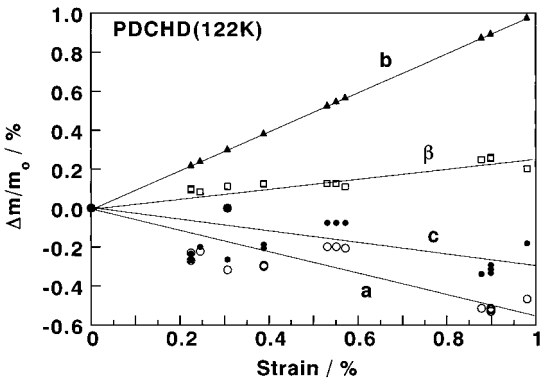

Figure 10. Stress-induced changes of lattice parameters obtained at 122 K.

estimate the so-called Poisson's ratios as follows:

$$\nu_{c'b} = -(\Delta c'/c'_o)/(\Delta b/b_o) = -(\Delta c \sin\beta/c_o \sin\beta)/(\Delta b/b_o) = 0.67$$

$$\nu_{ab} = -(\Delta a/a_o)/(\Delta b/b_o) = 0.38$$

where the c' is the component of the *c* axis perpendicular

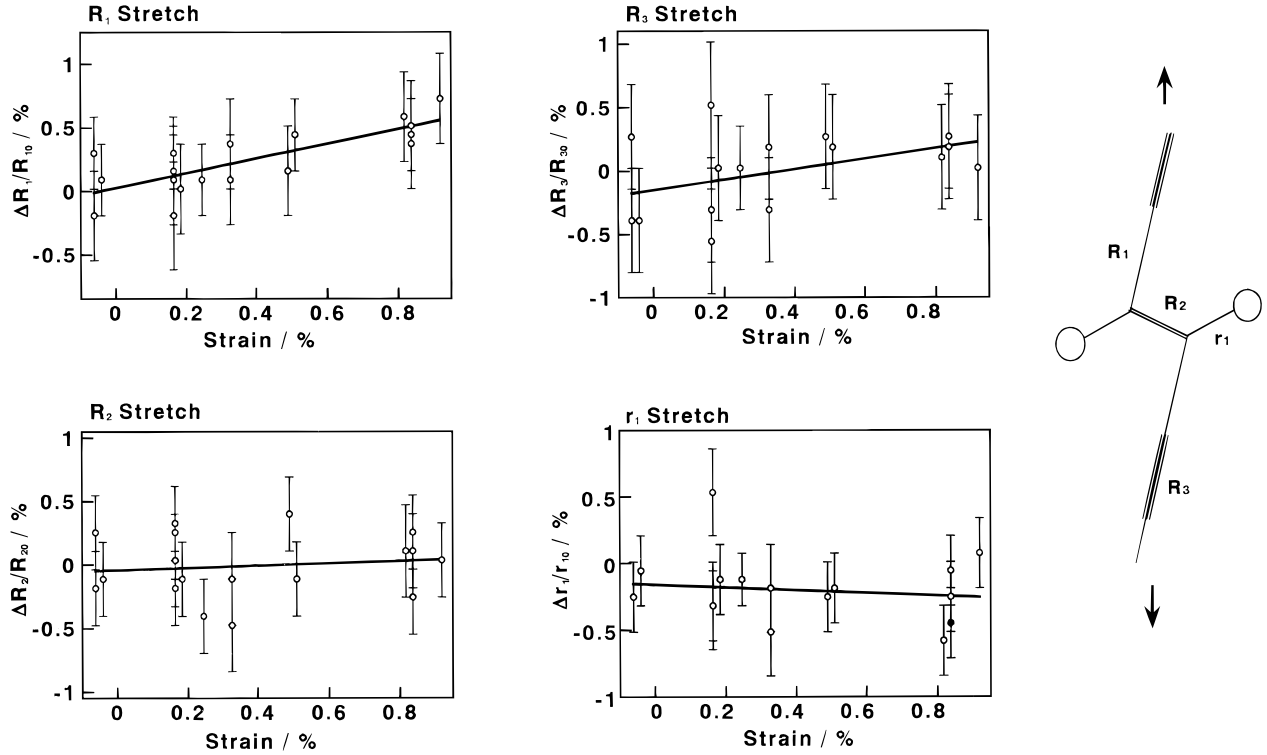

Figure 11. Strain dependence of bond lengths of the PDCHD chain (122 K). The definition of the bond lengths is made in the right side of this figure.

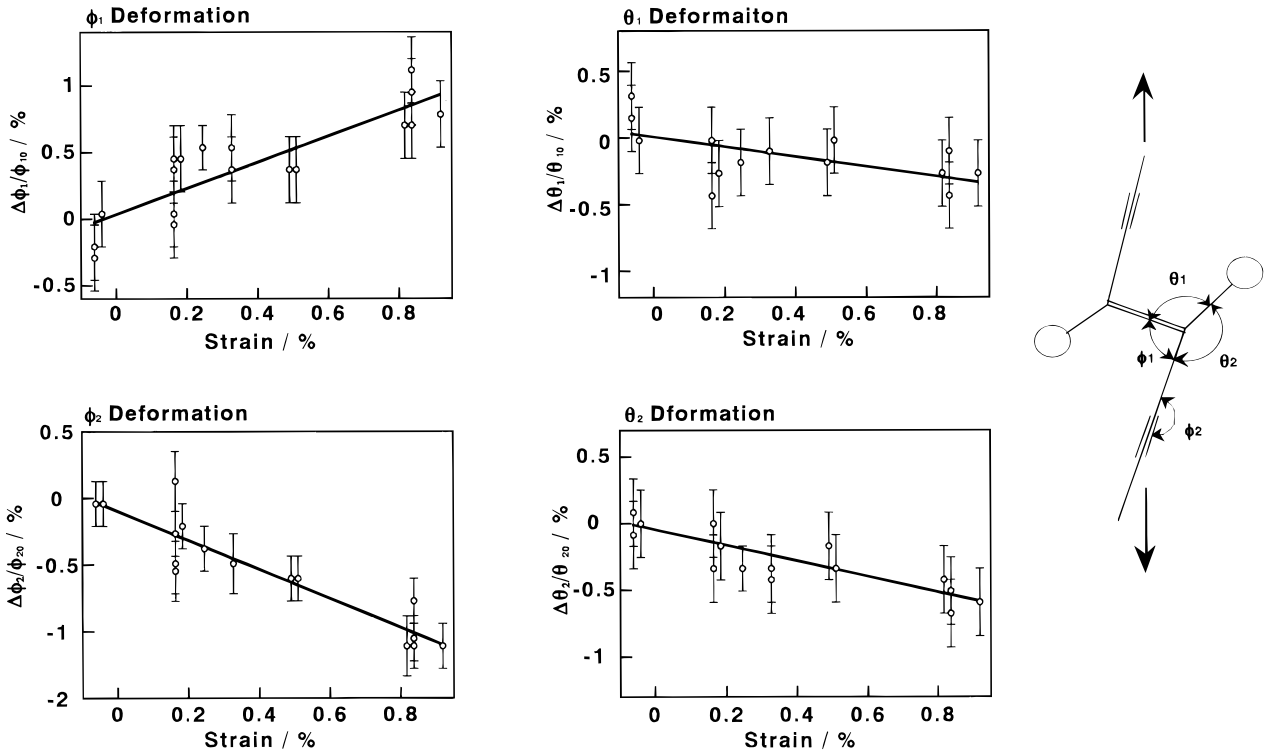

Figure 12. Strain dependence of bond angles of the PDCHD chain (122 K). The definition of the bond angles is made in the right side of this figure.

to the *a* axis and the angle β is practically constant. Such an exact evaluation of the Poisson's ratio of the polymer crystal is considered to be the first case as long as the authors know. Of course the Poisson's ratio of polymer "crystallites" had been reported for orthorhombic polyethylene (PE), for example, by measuring the stress-induced shift of the X-ray reflectional position.[22,23] However, the evaluated Poisson's ratio depends on the sample preparation condition and fluctuates in a remarkably wide range of the value: for example, the ratios of 1.6−3.8 were reported for ν_{ac} and ν_{bc} of the normally oriented PE samples annealed at the various temperatures and the values 0.2−0.7 for ν_{ac} of the ultradrawn PE sample with large experimental errors. Miyasaka et al. ascribed the anomalous high Poisson's ratio of the former case to the coupling between the original compression of the unit cell of the crystalline region and the additional compression of the cell caused by a deformation of amorphous phase contact with the crystalline region.[22] In the latter case of the ultradrawn

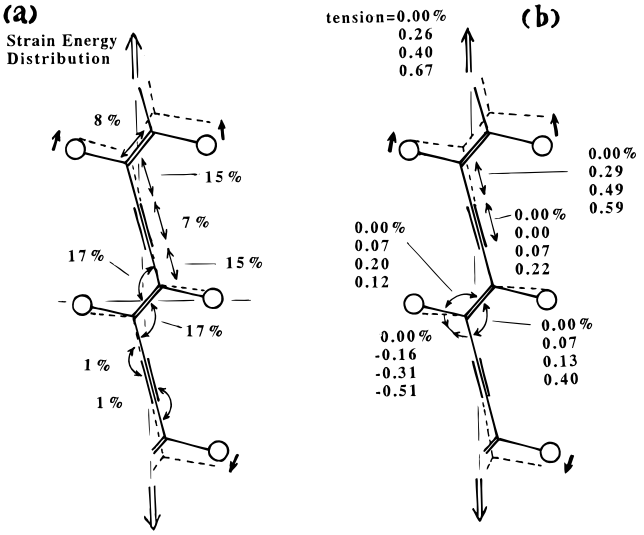

Figure 13. (a) Lattice-dynamically calculated molecular deformation and the strain energy distribution to the various internal coordinates of the PDCHD skeletal chain;[8] (b) X-ray analyzed changes of the internal coordinates of the PDCHD skeletal chain. Four rows of strain percentages shown at each internal coordinate correspond to the four stages of tension (from 0.0 to 0.67%).

PE sample, the sample is almost purely crystalline, and the measured ratios may be relatively closer to the true ones but the observable reflections are too small in number to evaluate the infinitesimally small change in the lattice constants quantitatively exactly.

Chain Deformation and Geometrical Changes. (A) At Room Temperature. All of the X-ray diffraction data thus collected were utilized in the refined structure analyses. The changes in the structural parameters of the molecular chains are plotted against the strain in Figures 7 and 8. As shown in Figure 7, the bond lengths of the skeletal chains R_1(C—C) and R_3-(C≡C) are stretched almost linearly with an increase of tensile strain, while the bond length R_2(C═C) and the r_1 (the bond length between the skeletal chain atom and the side-group atom CH_2) are decreased to some extent. The bond length r_2 in the side group does not change at all. In Figure 8, the bond angle ϕ_1(<CC═C) of the skeletal zigzag chain increases but the angle θ_2 (between the bonds R_1 and r_1) decreases so as to compensate the increment of these angles ϕ_1 and θ_1. The increase of the bond lengths and bond angles of the planar-zigzag skeletal chain subjected to the tensile stretching field may be easily imagined. The skeletal angle ϕ_2 is the angle <CC≡C of an almost linear part of the skeletal zigzag chain (178.9° at the free strain state). This angle is decreased when the chain is stretched, meaning that the long virtual bond of CC≡CC is bent and wound slightly under tension. The inner structure of the side groups shows almost no geometrical change during the tensile deformation, although the orientation of the carbazolyl groups is changed slightly as a result of the skeletal chain deformation and also due to the compression from the surrounding chains.

Figure 9 shows the tensile strain dependence of the diagonal components of the anisotropic thermal parameters u_{ii}. The experimental error of the thermal factors is not so small as compared with that of the geometrical parameters, making a quantitative discussion difficult. But, as a general tendency, the thermal vibrations of the atoms in the lateral *a* and *c* directions seem to be depressed relatively largely compared with those along the chain axis. This may be reasonable if we imagine

Table 2. Fractional Coordinates and Equivalent Temperature Factors of Atoms of PDCHD in the Strain Free State[a]

atom[b]	*x*/*a*	*y*/*b*	*z*/*c*	*U*(iso)/Å^2
C(1)	0.009 34(15)	0.120 34(42)	0.006 00(14)	0.040
C(2)	0.034 40(14)	0.399 89(42)	0.021 29(13)	0.037
C(3)	0.141 90(17)	0.480 60(50)	0.085 65(16)	0.050
C(4)	0.192 00(18)	0.183 31(51)	0.210 86(16)	0.049
C(5)	0.268 43(19)	−0.023 73(53)	0.243 87(17)	0.053
C(6)	0.275 4(3)	−0.137 9(7)	0.319 2(2)	0.080
C(7)	0.208 0(4)	−0.038 4(10)	0.360 1(3)	0.107
C(8)	0.134 4(3)	0.171 5(9)	0.327 9(2)	0.100
C(9)	0.124 2(2)	0.286 2(7)	0.252 3(2)	0.077
C(10)	0.280 31(16)	0.096 44(49)	0.119 96(16)	0.048
C(11)	0.324 34(16)	−0.078 53(53)	0.185 28(17)	0.052
C(12)	0.406 9(2)	−0.263 5(6)	0.182 9(2)	0.072
C(13)	0.440 7(2)	−0.268 6(8)	0.116 0(3)	0.105
C(14)	0.394 6(3)	−0.095 3(8)	0.050 8(3)	0.098
C(15)	0.313 6(2)	0.092 4(7)	0.050 8(2)	0.072
N(1)	0.199 64(13)	0.257 49(38)	0.135 22(12)	0.044
H(3A)	0.125 70	0.615 80	0.120 45	0.09(1)
H(3B)	0.189 30	0.559 90	0.058 55	0.073(8)
H(15)	0.282 54	0.213 19	0.005 76	0.079(9)
H(14)	0.421 52	−0.106 65	0.005 11	0.08(1)
H(13)	0.495 72	−0.398 05	0.113 32	0.09(1)
H(12)	0.439 85	−0.384 51	0.227 51	0.10(1)
H(6)	0.322 81	−0.290 86	0.339 90	0.14(2)
H(7)	0.215 82	−0.109 89	0.413 16	0.13(1)
H(8)	0.089 41	0.234 46	0.359 23	0.11(1)
H(9)	0.072 78	0.430 14	0.229 80	0.066(8)

[a] The lattice parameters are a = 12.846 Å, b = 4.887 Å, c = 17.332 Å, and β = 108.30°. Equivalent thermal parameters U(iso) = $(4/3)\sum_{ij}U_{ij}(\mathbf{a}_i\cdot\mathbf{a}_j)$ where $\mathbf{a}_i$ and $\mathbf{a}_j$ are the unit cell vectors (i, j = 1, 2, and 3). U_{ij} are the components of the anisotropic temperature factors (Supporting Information). For the hydrogen atoms, the isotropic thermal factors were determined. [b] The numbering of the atoms is shown as follows. The numbering of the hydrogen atoms follows that of the non-hydrogen atoms.

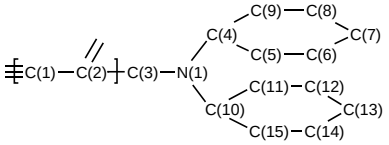

that the thermal vibrations of the chains are restricted to some extent in the lateral directions due to the compression of the unit cell in this direction, as shown in Figure 6.

(B) At Low Temperature. Similar experiments were also carried out at low temperature. This was because the thermal vibrations of atoms are depressed at low temperature, so we may expect to obtain more refined evaluation of stress-induced atomic displacements without any disturbance due to such a thermal motion. The sample was cooled by blowing the cooled nitrogen gas by using a Cryostream Cooler (Oxford Cryosystems Co. Ltd.). The temperature at the sample position was 122 K as measured by a thermoelectric couple. The sample was placed under tension and cooled to 122 K, and the X-ray diffraction was measured in the same way as that described in the previous section.

The averaged lattice parameters at 122 K were as follows: $\langle a\rangle$ = 12.647 Å, $\langle b\rangle$ = 4.899 Å, $\langle c\rangle$ = 17.127 Å, and $\langle\beta\rangle$ = 108.28°. At low temperature the cell parameters in the lateral direction are contracted largely, the chain axis (*b* axis) is increased, and the angle β is not changed very much. The expansion of the *b*-axial length is due to the decrease of thermal fluctuation of the molecular chain at low temperature as is well-known for many polymer crystals. This change in the cell constants induces the change in the internal parameters

Table 3. Internal Coordinates of PDCHD Chain at the Strain Free State[a]

	Bond Lengths (Å)		
C(1)−C(1)	1.205(3)	C(1)−C(2)	1.409(3)
C(2)−C(2)	1.369(3)	C(2)−C(3)	1.530(3)
C(3)−N(1)	1.441(4)	C(4)−C(5)	1.401(4)
C(4)−C(9)	1.386(5)	C(4)−N(1)	1.393(4)
C(5)−C(6)	1.397(5)	C(5)−C(11)	1.441(4)
C(6)−C(7)	1.368(7)	C(7)−C(8)	1.387(7)
C(8)−C(9)	1.394(6)	C(10)−C(11)	1.389(4)
C(10)−C(15)	1.395(5)	C(10)−N(1)	1.391(3)
C(11)−C(12)	1.403(4)	C(12)−C(13)	1.361(7)
C(13)−C(14)	1.387(7)	C(14)−C(15)	1.387(5)
	Bond Angles (deg)		
C(1)−C(1)−C(2)	178.3(3)	C(1)−C(2)−C(2)	121.4(2)
C(1)−C(2)−C(3)	119.2(2)	C(2)−C(2)−C(3)	119.4(2)
C(2)−C(3)−N(1)	114.7(2)	C(5)−C(4)−C(9)	121.6(3)
C(5)−C(4)−N(1)	109.0(3)	C(9)−C(4)−N(1)	129.4(3)
C(4)−C(5)−C(6)	120.1(3)	C(4)−C(5)−C(11)	106.7(3)
C(6)−C(5)−C(11)	133.2(3)	C(5)−C(6)−C(7)	118.5(4)
C(6)−C(7)−C(8)	121.1(4)	C(7)−C(8)−C(9)	121.7(4)
C(4)−C(9)−C(8)	116.9(4)	C(11)−C(10)−C(15)	122.4(3)
C(11)−C(10)−N(1)	109.3(3)	C(15)−C(10)−N(1)	128.3(3)
C(5)−C(11)−C(10)	107.1(3)	C(5)−C(11)−C(12)	133.5(3)
C(10)−C(11)−C(12)	119.4(3)	C(11)−C(12)−C(13)	118.9(4)
C(12)−C(13)−C(14)	120.9(4)	C(13)−C(14)−C(15)	122.2(4)
C(10)−C(15)−C(14)	116.2(4)	C(3)−N(1)−C(4)	125.6(2)
C(3)−N(1)−C(10)	126.1(2)	C(4)−N(1)−C(10)	108.0(2)
	Torsional Angles (deg)		
C(1)−C(1)−C(2)−C(3)	−14.3(76)	C(1)−C(2)−C(3)−N(1)	−10.4(2)
C(2)−C(2)−C(3)−N(1)	170.9(3)	C(2)−C(3)−N(1)−C(4)	−94.8(3)
C(2)−C(3)−N(1)−C(10)	92.0(3)	C(9)−C(4)−C(5)−C(6)	2.0(3)
C(5)−C(4)−C(9)−C(8)	−0.9(3)	C(9)−C(4)−C(5)−C(11)	−179.7(4)
C(5)−C(4)−N(1)−C(3)	−173.9(4)	N(1)−C(4)−C(5)−C(6)	−178.7(4)
C(5)−C(4)−N(1)−C(10)	0.4(3)	N(1)−C(4)−C(5)−C(11)	−0.4(2)
C(9)−C(4)−N(1)−C(3)	5.4(3)	N(1)−C(4)−C(9)−C(8)	180.0(5)
C(9)−C(4)−N(1)−C(10)	179.6(4)	C(4)−C(5)−C(6)−C(7)	−1.5(4)
C(4)−C(5)−C(11)−C(10)	0.2(3)	C(4)−C(5)−C(11)−C(12)	−178.9(5)
C(11)−C(5)−C(6)−C(7)	−179.2(6)	C(6)−C(5)−C(11)−C(10)	178.2(5)
C(6)−C(5)−C(11)−C(12)	−0.9(4)	C(5)−C(6)−C(7)−C(8)	−0.2(4)
C(6)−C(7)−C(8)−C(9)	1.3(4)	C(7)−C(8)−C(9)−C(4)	−0.8(4)
C(15)−C(10)−C(11)−C(5)	−178.1(4)	C(15)−C(10)−C(11)−C(12)	1.2(3)
C(11)−C(10)−C(15)−C(14)	−0.6(3)	C(11)−C(10)−N(1)−C(3)	174.0(4)
C(11)−C(10)−N(1)−C(4)	−0.3(2)	N(1)−C(10)−C(11)−C(5)	0.0(2)
N(1)−C(10)−C(11)−C(12)	179.3(4)	C(15)−C(10)−N(1)−C(3)	−8.1(3)
C(15)−C(10)−N(1)−C(4)	177.7(4)	N(1)−C(10)−C(15)−C(14)	−178.3(5)
C(5)−C(11)−C(12)−C(13)	178.3(6)	C(10)−C(11)−C(12)−C(13)	−0.8(4)
C(11)−C(12)−C(13)−C(14)	−0.2(4)	C(12)−C(13)−C(14)−C(15)	0.9(4)
C(13)−C(14)−C(15)−C(10)	−0.4(4)		

Mean Planes[b]

plane atoms	x_i	y_i	z_i
C(4)	−1.2436	0.4675	−0.0021
C(5)	−0.7920	−0.8584	0.0124
C(6)	−1.7095	−1.9109	−0.0185
C(7)	−3.0449	−1.6122	−0.0322
C(8)	−3.4859	−0.2969	−0.0127
C(9)	−2.5951	0.7750	−0.0053
C(10)	1.0076	0.5378	0.0135
C(11)	0.6483	−0.8044	0.0188
C(12)	1.6519	−1.7854	0.0130
C(13)	2.9546	−1.3936	−0.0135
C(14)	3.2946	−0.0487	−0.0396
C(15)	2.3380	0.9552	−0.0226
N(1)	−0.1423	1.3208	0.0042

[a] The numbering of atoms is referred to in Table 2. [b] x_i, y_i, and z_i are the coordinates with respect to the inertial axes. z_i represents the atomic displacement from the mean plane.

of the molecular chain: the skeletal bond length R_1-(C−C) and R_3(C≡C) are increased, the R_2(C═C) is not changed at all, and the skeletal bond angle ϕ_1 is deceased at low temperature.

When the crystal was stretched at a constant strain at low temperature, the averaged lattice parameters are changed, as plotted in Figure 10. Although the details are different from the case obtained at room temperature, the essential feature of the change in the cell parameters is almost the same. This can be said also for the changes in the molecular parameters, as shown in Figures 11 and 12. When these data obtained at 122 K are compared with those at 294 K, the essential features of the mechanical deformation of the molecular chain are found also to be essentially the same, although the starting geometry of the chain at the free strain state is slightly different from each other at these two temperatures. In this way, the structural analyses made at low temperature can make us reconfirm definitely the mechanical deformation mechanism of the

molecular chain clarified at room temperature. The detailed discussion about the difference in the structural data obtained at two different temperatures will be made in a separate paper.

Comparison of the X-ray Analyzed Deformation Mechanism with the Lattice-Dynamical Prediction. Several years ago we predicted the atomic displacements occurring in the strained PDCHD chain on the basis of the lattice dynamical theory.[8] In Figure 13a is shown the theoretical calculation of the deformation of the skeletal chain and the distribution of the strain energy to the various internal coordinates. The planar-zigzag chain is stretched so as to become straight along the chain axis. The strain energy distributes preferentially to the change of the skeletal chain conformation: in particular the distribution to the stretching of the skeletal C—C, C═C, and C≡C bonds and the opening of the angle <C═CC is significant. This type of chain deformation is qualitatively in good coincidence with the above-mentioned conformational change [see Figure 13b where the changes of the parameters are listed correspondingly to the increase of the tension from 0.0 to 0.67%], although the quantitative comparison is still difficult at present because the force field employed in the theoretical calculation was too simplified.[8] We will be carrying out the more detailed molecular mechanics and quantum chemical calculations of the PDCHD crystal subjected to the tensile stress. However, we may say that the X-ray structural analysis has been for the first time able to confirm experimentally the molecular deformation mechanism of the PDCHD chain which was predicted theoretically on the basis of the lattice-dynamical calculation.

Concluding Remarks

In this paper we have described the atomic displacements or the molecular deformation mechanism of the planar-zigzag PDCHD chain subjected to the tensile stress through the refined X-ray structural analysis based on the reflectional data collected by the IP system. Beyond the experimental errors the bond lengths and bond angles of the skeletal chains have been found to change systematically with the extension of the chain axial length. The thus revealed deformation mechanism was found to correspond fairly well to the lattice-dynamical prediction result, although a more quantitative comparison is needed in the future. This type of X-ray structural analysis may be the first success in clarifying the molecular deformation behavior of a synthetic polymer single crystal. If we can collect this type of information for many crystalline polymers, it may serve quite usefully in the discussion of the intimate relationship between the structural deformation mechanism and the mechanical property of polymers as viewed from the molecular level.

Acknowledgment. The authors wish to thank Mr. Yukihiro Shimura and Mr. Naomi Shimura of MAC Science Co. Ltd., and Dr. Chuji Katayama, the research institute of MAC Science Co. Ltd., for their heartfelt encouragement and kind advice in carrying out the X-ray structural analysis. This work was supported by a Grant-in-Aid for Special Scientific Research "Analytical System of Dynamic Structures" of the Ministry of Education, Science, and Culture of Japan.

Supporting Information Available: Tables of the comparison of the molecular parameters of cytidine among the various data obtained by the different installments, of the temperature factors of the constituent atoms of PDCHD at the free strain state, and of the *R*-factor, R_w-factor, the number of the observed unique reflections, and the numbers of the reflections used in the structural refinements for all of the PDCHD crystals used in the experiments (3 pages). Ordering information is given on any current masthead page.

References and Notes

(1) Tashiro, K. *Prog. Polym. Sci.* **1993**, *18*, 377.
(2) Wool, R. P.; Bretzlaff, R. S.; Li, B. Y.; Wang, C. H.; Boyd, R. H. *J. Polym. Sci., Polym. Phys. Ed.* **1986**, *24*, 1039.
(3) Day, R. J.; Robinson, I. M.; Zakikhani, M.; Young, R. J. *Polymer* **1987**, *28*, 1833.
(4) Mitra, V. K.; Risen, W.; Baughman, R. H. *J. Chem. Phys.* **1977**, *66*, 2731.
(5) Batchelder, D. N.; Bloor, D. *J. Polym. Sci., Polym. Phys. Ed.* **1979**, *17*, 569.
(6) Bretzlaff, R. S.; Wool, R. P. *Macromolecules* **1983**, *16*, 1907.
(7) Wu, G.; Tashiro, K.; Kobayashi, M.; Komatsu, T.; Nakagawa, K. *Macromolecules* **1989**, *22*, 758.
(8) Wu, G.; Tashiro, K.; Kobayashi, M. *Macromolecules* **1989**, *22*, 188.
(9) Tashiro, K.; Wu, G.; Kobayashi, M. *J. Polym. Sci., Part B: Polym. Phys.* **1990**, *28*, 2527.
(10) Tashiro, K.; Minami, S.; Wu, G.; Kobayashi, M. *J. Polym. Sci., Part B: Polym. Phys.* **1992**, *30*, 1143.
(11) Tashiro, K.; Wu, G.; Kobayashi, M. *Polymer* **1988**, *29*, 1768.
(12) Tashiro, K.; Kobayashi, M.; Tadokoro, H. *Polym. Eng. Sci.* **1994**, *34*, 308.
(13) Otwinowski, Z. *Proceedings of the CCP4 Study Weekend: Data Collection and Processing*, Jan 29—30 1993; Sawyer, L., Isaacs, N., Bailey, S., Eds.; SERC Daresbury Laboratory: Daresbury, England, 1993; p 56.
(14) Minor, W. *XDISPLAYF Program;* Purdue University: Lafayette, IN, 1993.
(15) Otwinowski, Z.; Minor, W. *The HKL Program Suite*, in press.
(16) Main, P.; Lessinger, L.; Woolfsom, M. M.; Germain, G.; Declercq, J. P. *Multan 78* (A system of computer programs for the automatic solution of crystal structures from X-ray diffraction data); University of York: York, England, and Louvain, Belgium, 1976.
(17) Miyahara, J.; Takahashi, K.; Amemiya, Y.; Kamiya, N.; Satow, Y.; *Nucl. Instrum. Methods Phys. Res.* **1986**, *A246*, 572.
(18) Sakabe, N.; Nakagawa, K.; Sasaki, K.; Watanabe, N. *Rev. Sci. Instrum.* **1989,** *60*, 2440.
(19) Amemiya, Y.; Wakabayashi, K.; Tanaka, H.; Ueno, U.; Miyahara, J. *Science* **1987**, *237*, 164.
(20) Furberg, S.; Petersen, C. S.; Romming, Chr. *Acta Crystallogr.* **1965**, *18*, 313.
(21) Apgar, P. A.; Yee, K. C. *Acta Crystallogr.* **1978**, *B34*, 957.
(22) Miyasaka, K.; Makishima, K. *Kobunshi Kagaku (Polym. Chem.)* **1966**, *23*, 785.
(23) Matsuo, M.; Okano, Y. *Polym. Prepr. Jpn.* **1994**, *43*, 1315.

MA960882F